Electronic Supplementary Material (ESI) for Journal of Materials Chemistry A.

A Lithium Sulfamate Layer with High Ionic Conductivity and Low Surface Diffusion Barrier Enabled Highly Reversible Lithium Metal Anode

Pinjuan Zou, Wenbin Jiang, Longtao Ma*, Liuzhang Ouyang*

School of Materials Science and Engineering, Guangdong Engineering Technology Research Center of Advanced Energy Storage Materials, South China University of Technology, Guangzhou, China

* Corresponding author. E-mail: longtaoma@scut.edu.cn

meouyang@scut.edu.cn

Experimental section

***Material synthesis*:** Sulfamic acid (SA) with a purity of > 99.5% was purchased from Aldrich and placed in an argon-filled glovebox. The metallic lithium foil (*Φ*15×0.5 mm) and lithium strip (50 μm in thickness) were purchased from China Energy Lithium Co., Ltd. Firstly, a certain amount of SA was dissolved in the dimethyl sulfoxide (DMSO, Macklin) solution under magnetic stirring. Afterwards, the Li plate was immersed in the SA/DMSO solution (0.025 M) for only few minutes and carefully brush away the residual liquid with a nonstick wiping paper. Then the treated Li foil was obtained by evaporating the solvent of DMSO at 80 °C overnight under Ar atmosphere. After the full reaction (HSO_3NH_2+ 2 Na =$NaSO_3NHNa$ + H_2), the as-obtained Li metal anode was labeled as Li-SA@Li. The electrodes were fabricated in an Ar-filled glovebox with H_2O and O_2 concentrations below 0.1 ppm.

***Material characterization*:** The morphology and elemental distribution of the Li anodes were carried out by field-emission scanning electron microscope (FE-SEM, Hitachi SU8010) with an energy dispersive X-ray spectroscope (EDS, JEOL JSM-6100LV). All the anodes after cycled were flushed with anhydrous 1,3-dioxolane (DOL) to remove residual Li salts and electrolyte in glovebox before operating. *In-situ* XRD analysis was tested on Bruker D8 Advanced (Cu Kα, λ=1.5418 Å) and studied by a specially made chamber. X-ray photoelectron spectroscopy (XPS, ESCALab220i-XL) with 300 W Al Kα radiations was performed to evaluate the chemical composition of the SEI layer. Optical microscope camera (Belona, 200X-800X) with Wi-Fi box was carried out to confirm the Li plating process.

Computational Details: Density function theory calculation were performed by using the CP2K package.1 PBE functional2 with Grimme D3 correction3 was used to describe the system. Unrestricted Kohn-Sham DFT has been used as the electronic structure method in the framework of the Gaussian and plane waves method.4, 5 The Goedecker-Teter-Hutter (GTH) pseudopotentials, 6, 7 DZVPMOLOPT-GTH basis sets4 were utilized to describe the molecules. A plane-wave energy cut-off of 500 Ry has been employed. Transition states along the reaction pathway were determined by using the climbing image nudged elastic band (CI-NEB) method. 8 Between the initial state and final state, seven images have been used to simulate the reaction pathway. The simulation is carried out within 17.593×9.859×16.000 A^3 three dimensional periodic cubic box.

***Electrochemical measurements*:** CR-2032 type coin cells were utilized to survey the electrochemical performances of the as-prepared electrodes. 1 M LiTFSI (Aldrich) dissolved in a mixture of DOL and DME (V:V 1:1) with 2wt% $LiNO_3$ as an additive was selected as the electrolyte and a 25 μm porous polypropylene based membrane (Celgard) was used as the separator. For the symmetric cell tests, two identical electrodes were tested under various current-capacity conditions to investigate the Li stripping/plating behavior. To prepare the Li-SA@Cu electrode, 40 μL of SA/DMSO solution was dripped onto the surface of Cu foil, and then one Li plate was placed on the surface of the modified Cu electrode and fixed with clamp. After shelving for 12 h, the Li-SA@Cu electrode was obtained after full stripped away up to 1.0 V at 0.5 mA cm^{-2}. For the CE testing, 1 mAh cm^{-2} Li metal was plated on Cu foil (Φ12 mm) and

then stripped away up to 1.0 V at various current densities for each cycle. For the full cell operations, the cells consisted of commercial $LiFePO_4$ cathode and Li or Li-SA@Li anode were cycled in 1.0 M $LiPF_6$ (EC:DMC:EMC, volume ratio 1:1:1) electrolyte at 0.5 C after activation at 0.1 C for 3 cycles in a voltage range of 2.5-4.2 V. Generally, the mass loading of the $LiFePO_4$ cathode is about 3-4 mg cm^{-2}, and the mass loading of the $LiNi_{0.8}Co_{0.1}Mn_{0.1}O_2$ cathode is about 7.5 mg cm^{-2} Electrochemical impedance spectroscopy (EIS) measurements were performed on an electrochemical workstation (CHI660a, Shanghai Chenhua) in the frequency ranging from 10^5 to 10^{-2} Hz.

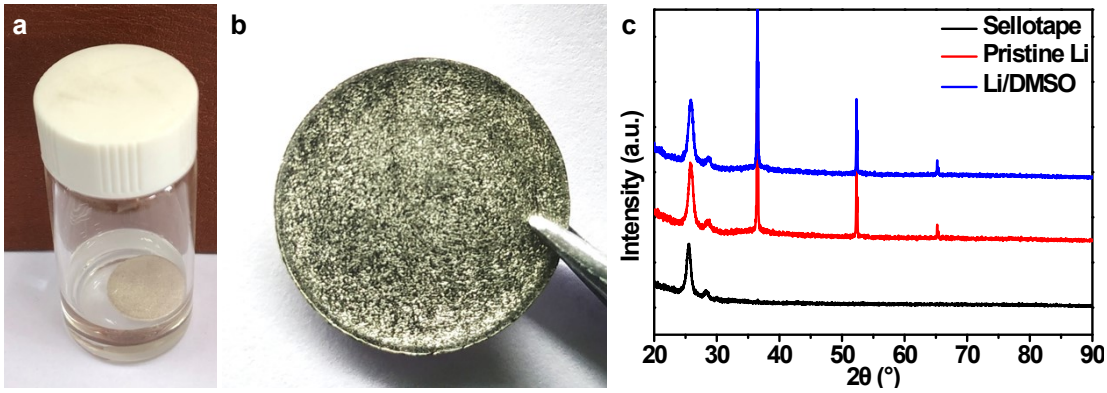

Figure S1. (a) Optical image of the reaction process between Li foil and 5 mL DMSO for 1 min and (b) the corresponding optical image of Li foil, (c) XRD patterns of Li foil after storage for 24 h.

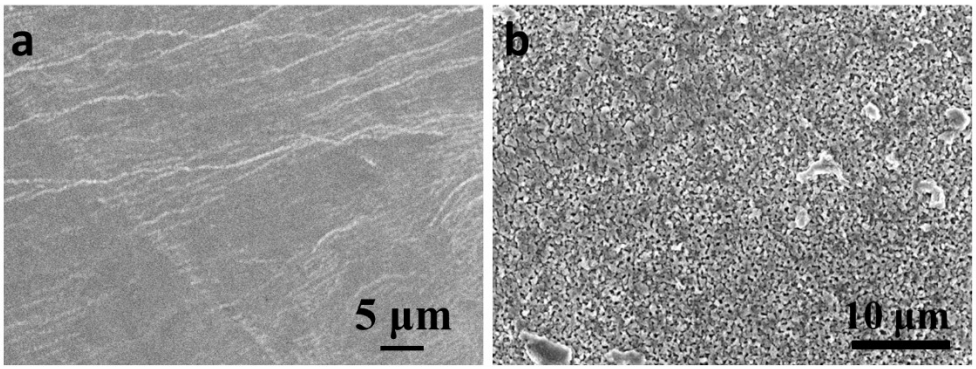

Figure S2. SEM images of (a) bare Li and (b) Li-SA@Li anode obtained by immersed in 0.15 M SA/DMSO solution

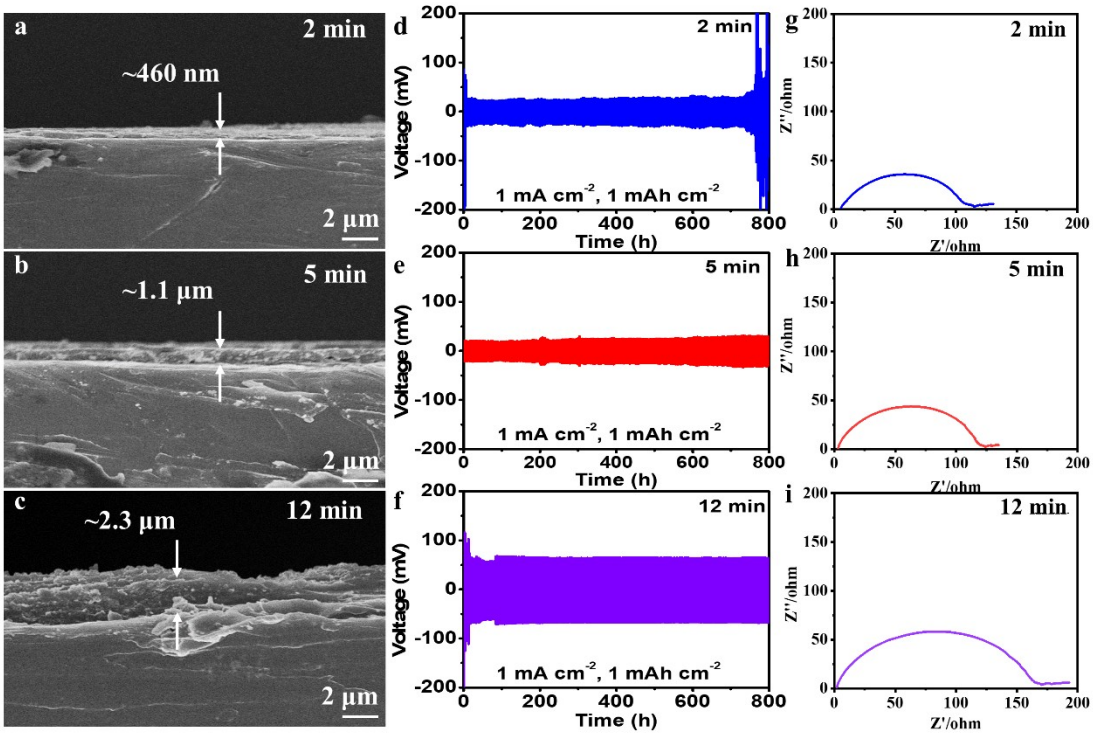

Figure S3. (a-c) The cross-sectional SEM images, (d-f) the corresponding cycling performances, and (g-i) the EIS curves of the Li-SA@Li metal anodes prepared by immersing in SA/DMSO solution for different time.

When the thickness of Li-SA layer was about 460 nm, the Li-SA@Li metal anode in the can keep stable cycling for 750 h in the Li symmetric cells with a voltage hysteresis of 27 mV. When the thickness of Li-SA layer was increased to about 1.1 μm, the Li-SA@Li metal anode in the can keep stable cycling for over 800 h in the Li symmetric cells with a voltage hysteresis of 30 mV. However, when the thickness of Li-SA layer was increased to about 2.3 μm, the voltage hysteresis of the Li symmetric cells was increased to 70 mV, although the Li symmetric cells can also maintain a stable cycling more than 800 h.

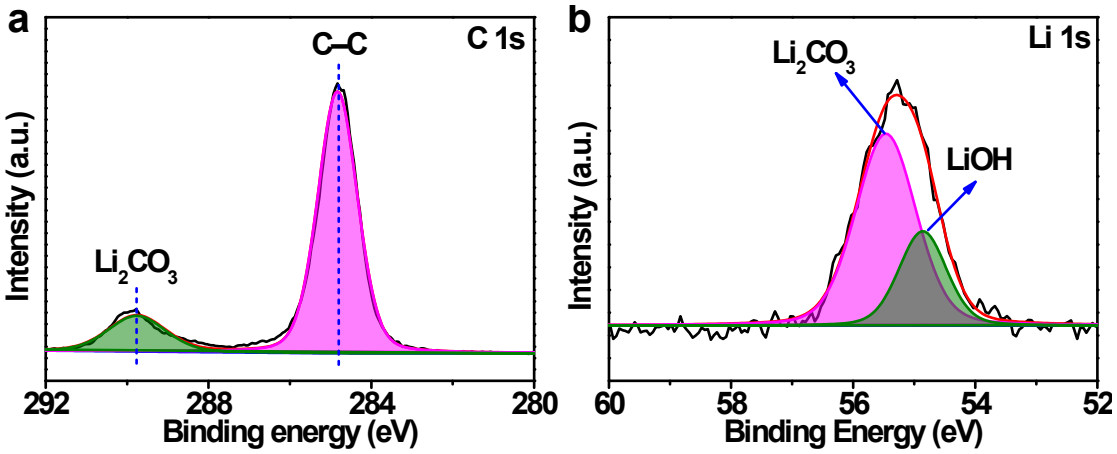

Figure S4. XPS analysis of (a) C 1s and (b) Li 1s for the pristine Li foil.

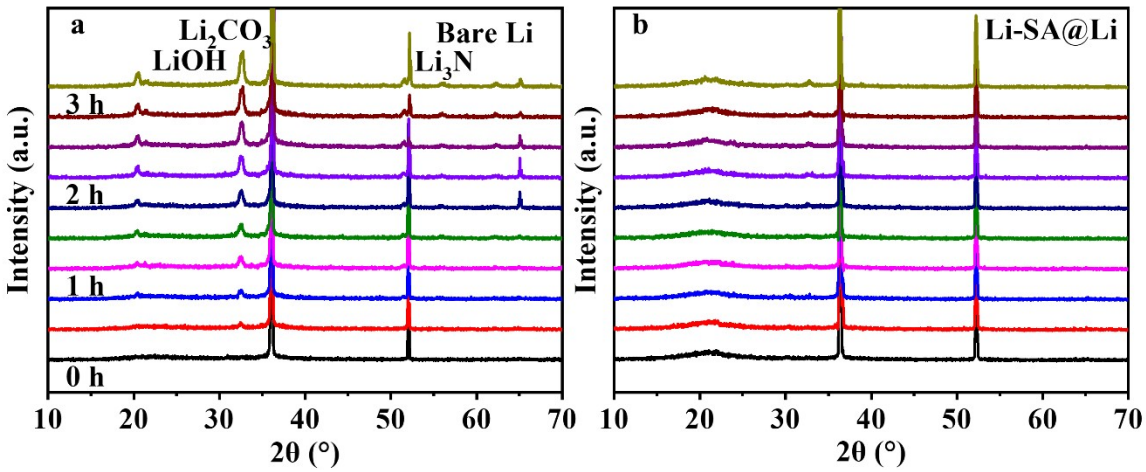

Figure S5. Continuous XRD patterns of (a) the bare Li and (b) Li-SA@Li foils exposed in air for different time.

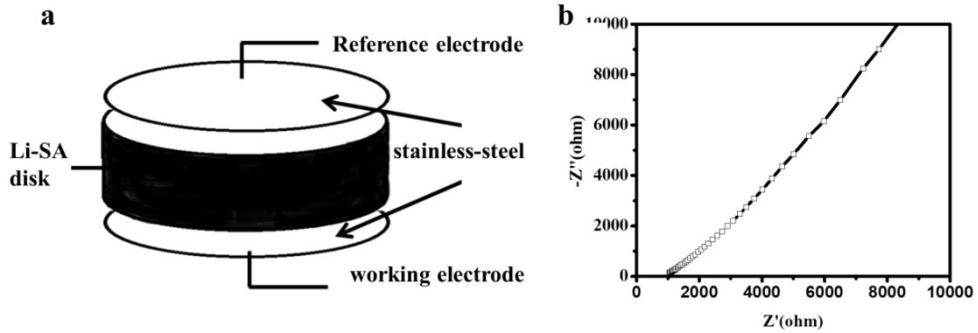

Figure S6. (a) the model of the symmetric SS|Li-SA|SS cell and (b) the corresponding EIS plot.

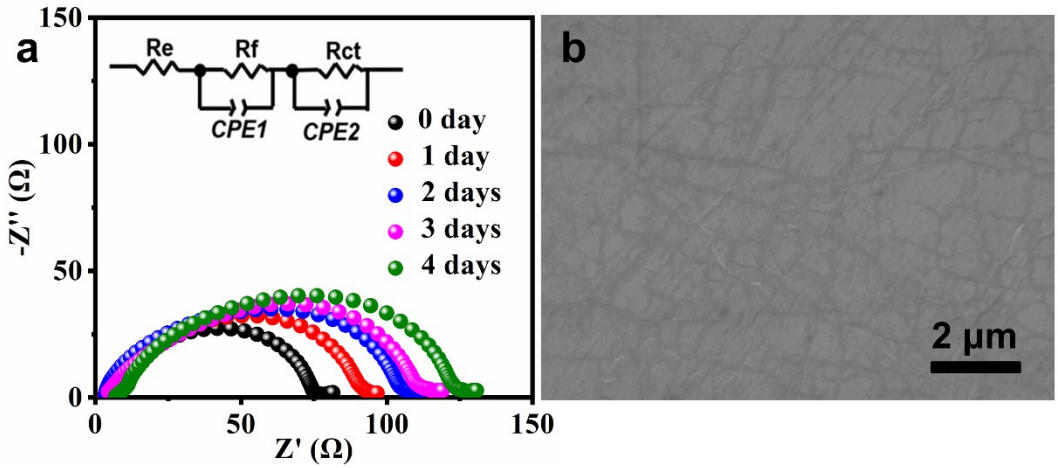

Figure S7. EIS evolution of (a) symmetric cells using Li anodes rest for different time at open circuit and (b) the SEM image of Li-SA@Li anode after storage in the electrolyte for 4 days.

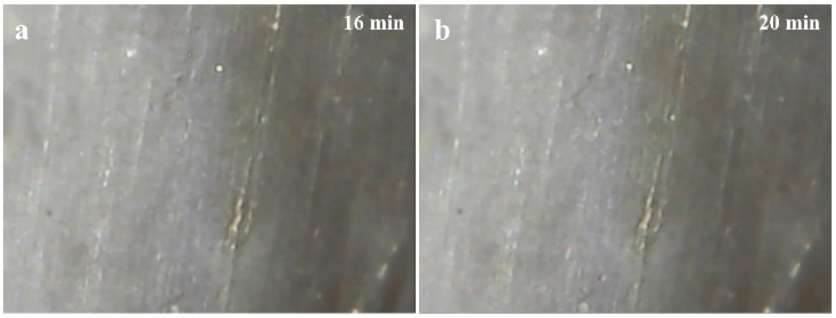

Figure S8. *In-situ* optical microscopy images of the Li deposition process for Li-SA@Li anode at different time at a current density of 4 mA cm^{-2}.

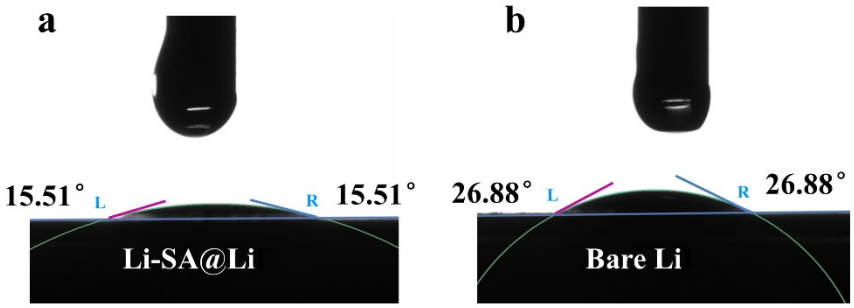

Figure S9. The contact angles between the electrolyte and (a)Li-SA@Li and (b) bare Li, respectively.

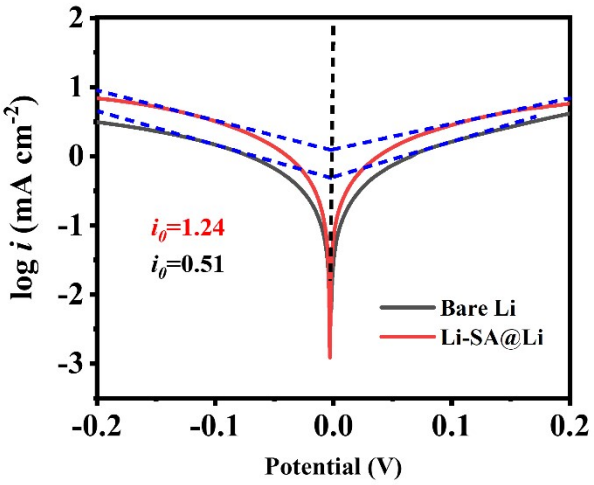

Figure S10. Tafel curves of (a) Li-SA@Li anode and (b) bare Li anode in the symmetric cells at a scan rate of 1.0 mV s^{-1}.

Table S1 Cycling stability comparison of the SA@Li anode with previously reported works on Li metal anodes.

Current density ($mA\ cm^{-2}$)	Deposition capacity ($mAh\ cm^{-2}$)	Overpotential (mV)	Cycle time (h)	References
0.5	0.5	20	580	Ref.9
0.5	1	20	1700	Ref.10
0.5	0.5	18	700	Ref.11
1	1	110	160	Ref.12
1	1	25	180	Ref.13
1	1	24	900	Ref.14
1	1	30	1200	Ref.15
1	1	36.3	800	Ref.16
1	1	28	1500	Ref.17
2	1	175	200	Ref.18
2	6	180	550	Ref.19
3	1	50	150	Ref.20
3	1	85	200	Ref.21
3	1	100	600	Ref.22
5	1	500	60	Ref.23
5	1	200	400	Ref.24
5	1	36	500	Ref.25
5	1	100	300	Ref.26
2	6	75	1500	
3	1	40	1600	This work
5		80	1200	

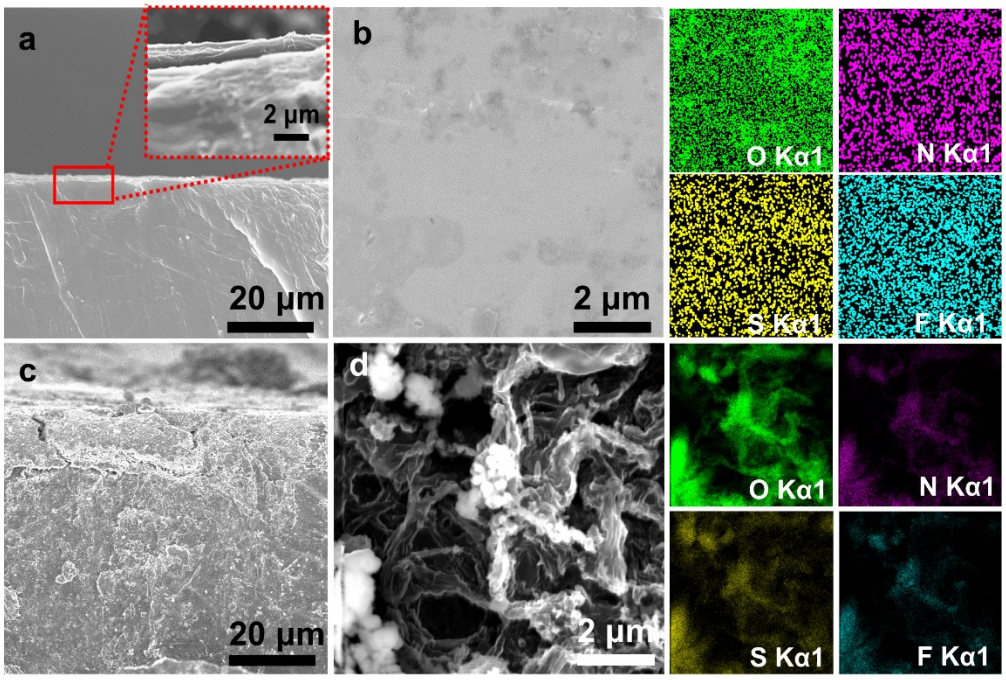

Figure S11. The cross-sectional SEM images of (a) Li-SA@Li anode (c) bare Li metal anode after 100 cycles in the symmetric cells. The EDS spectra of (b) Li-SA@Li anode and (d) bare Li anode after 100 cycles in symmetric cells.

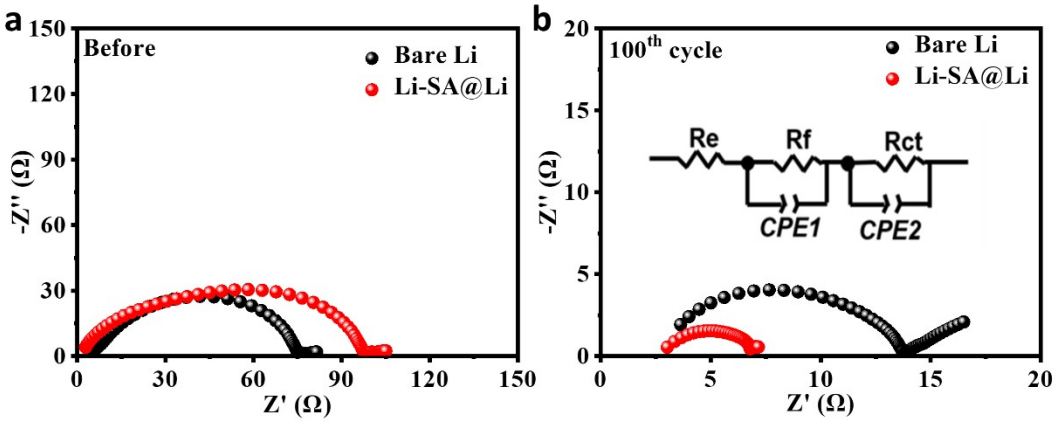

Figure S12. Nyquist plot of the impedance spectra of the bare and Li-SA@Li symmetric cells (a) before cycling and (b) after 100 cycles at 3 mA cm^{-2} under a fix capacity of 1 mAh cm^{-2}.

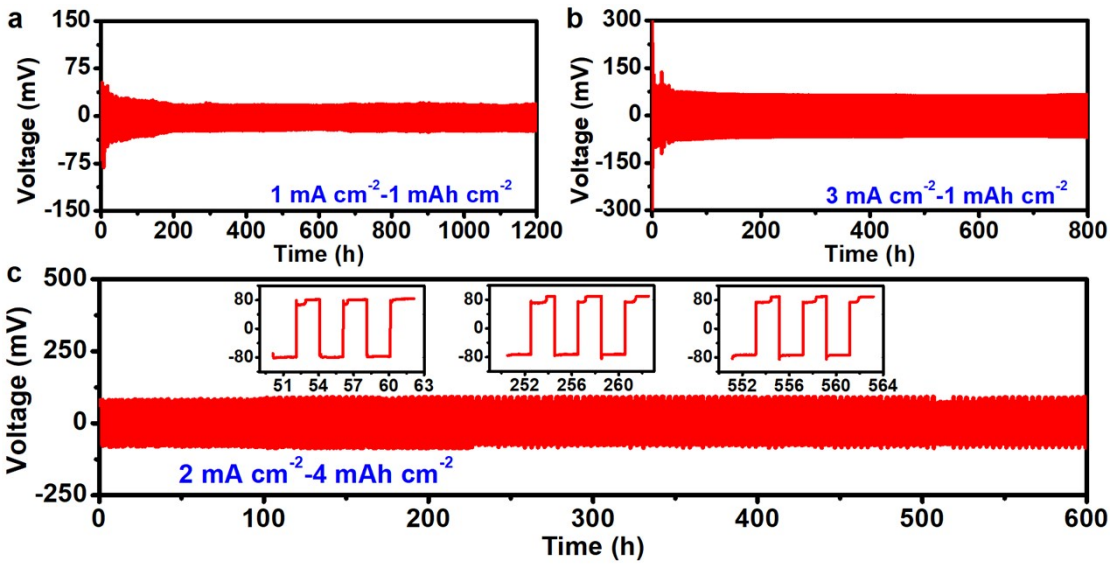

Figure S13. Cycling performances of Li-SA@Li with thickness of 50 μm in symmetric cells at a current density of (a) 1 mA cm^{-2} and (b) 3 mA cm^{-2} under 1 mAh cm^{-2}; (c) Cycling performances of Li-SA@Li using thin Li plate at 2 mA cm^{-2} under higher areal capacity of 4 mAh cm^{-2}.

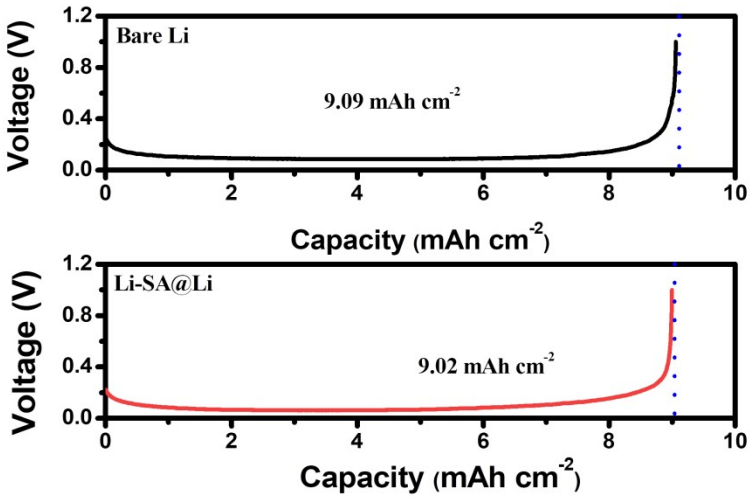

Figure S14. Typical Li stripping curve of (a) the bare thin Li anode and (b) Li-SA@Li anode (50 μm) at 1 mA·cm^{-2}.

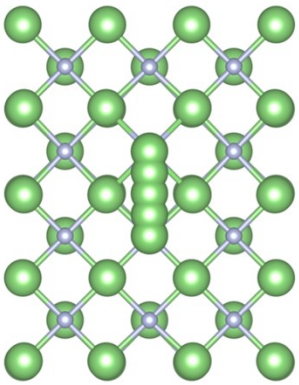

Figure S15. (a) The optimized Li-diffusion pathway on surface of LiF

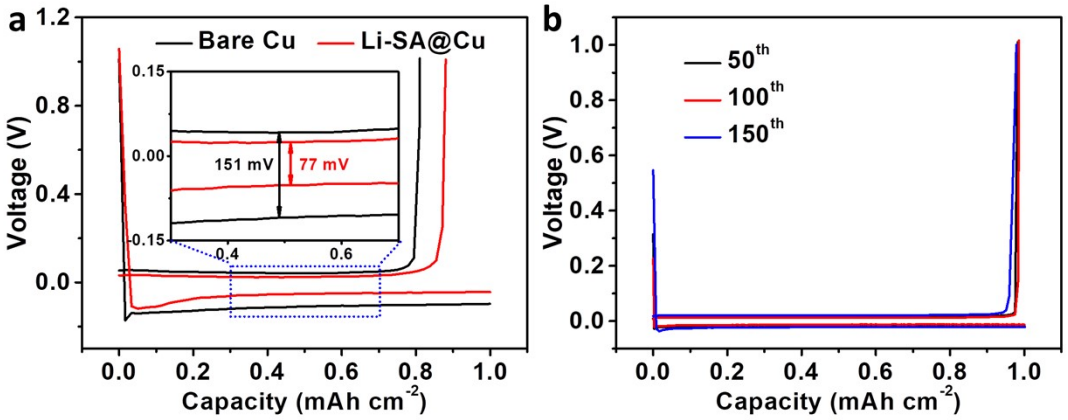

Figure S16. Comparison of the voltage profiles of Li plating/stripping on bare Cu and Li-SA@ Cu; (b) Polarization curves of Li plating/stripping on Li-SA@Li||Cu at different cycles.

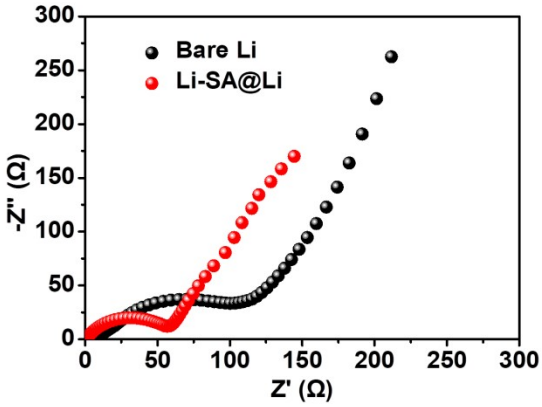

Figure S17. EIS of bare Li||LFP and Li-SA@Li||LFP full battery systems after 100 cycles.

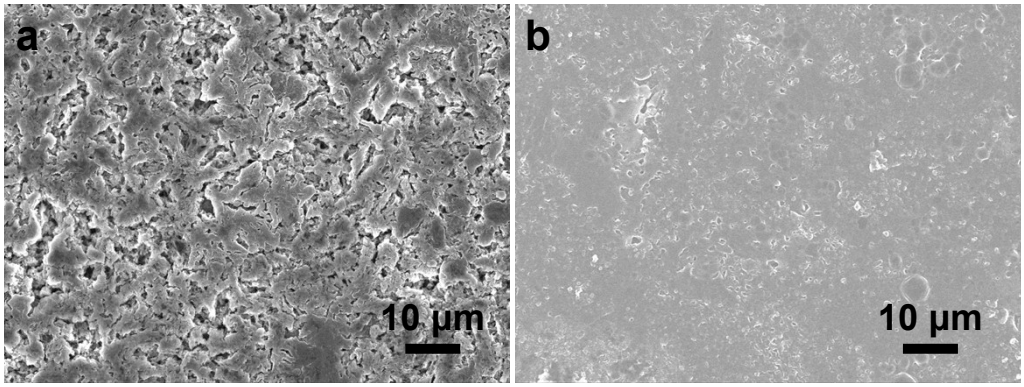

Figure S18. SEM images of (a) bare Li and (b) Li-SA@Li after 100 cycles in the Li||LFP full battery systems.

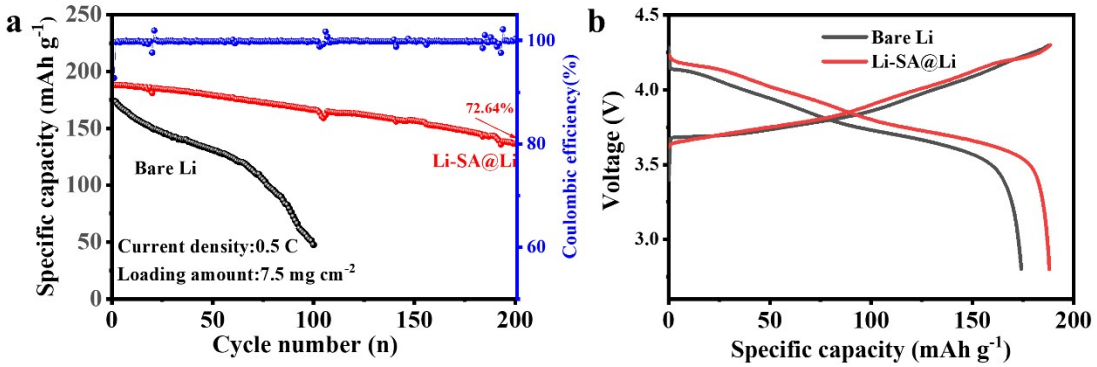

Figure S19. (a) The cycle stability of Li||NCM and Li-SA@Li||NCM at 0.5 C, and (b) the corresponding charge-discharge curves.

References

[1] J. r. Hutter, M. Iannuzzi, F. Schiffmann and J. Vandevondele, *Wiley Interdisciplinary Reviews: Computational Molecular Science*, 2014, **4**.
[2] J. P. Perdew, K. Burke and M. Ernzerhof, *Physical Review Letters*, 1996, **77**, 3865--3868.
[3] S. Grimme, *Journal of Computational Chemistry*, 2010, **27**, 1787-1799.
[4] J. Vandevondele and J. Hutter, *Journal of Chemical Physics*, 2007, **127**, 4365-4477.
[5] J. Vandevondele, M. Krack, F. Mohamed, M. Parrinello, T. Chassaing and J. Hutter, *Computer Physics Communications*, 2005, **167**, 103-128.
[6] S. Goedecker, M. Teter and J. Hutter, *Phys Rev B Condens Matter*, 1995, **54**, 1703-1710.
[7] C. Hartwigsen, S. Goedecker and J. Hutter, *Physical Review B*, 1998, **58**, 3641-3662.
[8] G. Henkelman, B. P. Uberuaga and H. Jo?Nsson, *The Journal of Chemical Physics*, 2000, **113**, 9901-9904.
[9] S. Wu, Z. Zhang, M. Lan, S. Yang, J. Cheng, J. Cai, J. Shen, Y. Zhu, K. Zhang and W. Zhang, *Advanced Materials*, 2018, **30**, 1705830.
[10] H. Ye, Z. J. Zheng, H. R. Yao, S. C. Liu, T. T. Zuo, X. W. Wu, Y. X. Yin, N. W. Li, J. J. Gu and F. F. Cao, *Angewandte Chemie International Edition*, 2019, **58**, 1094-1099.
[11] C. Zhang, W. Lv, G. Zhou, Z. Huang, Y. Zhang, R. Lyu, H. Wu, Q. Yun, F. Kang and Q.-H. Yang, *Advanced Energy Materials*, 2018, **8**, 1703404.
[12] L. Fan, H. L. Zhuang, L. Gao, Y. Lu and L. A. Archer, *Journal of Materials Chemistry A*, 2017, **5**, 3483-3492.
[13] F. Shen, F. Zhang, Y. Zheng, Z. Fan, Z. Li, Z. Sun, Y. Xuan, B. Zhao, Z. Lin, X. Gui, X. Han, Y. Cheng and C. Niu, *Energy Storage Materials*, 2018, **13**, 323-328.
[14] R. Song, Y. Ge, B. Wang, Q. Lv, F. Wang, T. Ruan, D. Wang, S. Dou and H. Liu, *Journal of Materials Chemistry A*, 2019, **7**, 18126-18134.
[15] S. Huang, W. Zhang, H. Ming, G. Cao, L.-Z. Fan and H. Zhang, *Nano Letters*, 2019, **19**, 1832-1837.
[16] D. Lee, S. Sun, H. Park, J. Kim, K. Park, I. Hwang, Y. Jung, T. Song and U. Paik, *Journal of Power Sources*, 2021, **506**, 230158.
[17] B. Han, Y. Zou, R. Ke, T. Li, Z. Zhang, C. Wang, M. Gu, Y. Deng, J. Yao and H. Meng, *ACS Applied Materials & Interfaces*, 2021, **13**, 21467-21473.
[18] Y. Chen, M. Yue, C. Liu, H. Zhang, Y. Yu, X. Li and H. Zhang, *Advanced Functional Materials*, 2019, **29**, 1806752.
[19] S. Li, X.-S. Wang, Q.-D. Li, Q. Liu, P.-R. Shi, J. Yu, W. Lv, F. Kang, Y.-B. He and Q.-H. Yang, *Journal of Materials Chemistry A*, 2021, **9**, 7667-7674.
[20] H. Qiu, T. Tang, M. Asif, X. Huang and Y. Hou, *Advanced Functional Materials*, 2019, **29**, 1808468.
[21] S. Liu, X. Xia, Y. Zhong, S. Deng, Z. Yao, L. Zhang, X.-B. Cheng, X. Wang, Q. Zhang and J. Tu, *Advanced Energy Materials*, 2018, **8**, 1702322.
[22] W. Wang, X. Yue, J. Meng, J. Wang, X. Wang, H. Chen, D. Shi, J. Fu, Y. Zhou, J. Chen and Z. Fu, *Energy Storage Materials*, 2019, **18**, 414-422.
[23] J. Lang, Y. Long, J. Qu, X. Luo, H. Wei, K. Huang, H. Zhang, L. Qi, Q. Zhang, Z. Li and H. Wu, *Energy Storage Materials*, 2019, **16**, 85-90.
[24] Y. Yuan, F. Wu, Y. Bai, Y. Li, G. Chen, Z. Wang and C. Wu, *Energy Storage Materials*, 2019, **16**, 411-418.
[25] F. Liu, R. Xu, Z. Hu, S. Ye, S. Zeng, Y. Yao, S. Li and Y. Yu, *Small*, 2019, **15**, 1803734.
[26] G. Jiang, K. Li, F. Yu, X. Li, J. Mao, W. Jiang, F. Sun, B. Dai and Y. Li, *Advanced Energy Materials*, 2021, **11**, 2003496.